Persistent Scatterer Interferometry in the Post-Event Monitoring of the Idukki Landslides

Journal:	*Geocarto International*
Manuscript ID	TGEI-2020-0103.R1
Manuscript Type:	Original Article
Keywords:	Sentinel-1, landslide monitoring, Idukki landslide, PS-InSAR, remote sensing

Persistent Scatterer Interferometry in the Post-Event Monitoring of the Idukki Landslides ~~in August 2018~~

Abstract

The monitoring of pre-failure movements and their evolution over time is necessary to assess the predisposing and triggering factors. This research focusses on assessing terrain displacements in the Idukki district (Kerala, India) over a year before the deadly disaster, which occurred in August 2018; this disaster was claimed to be a dreadful one as it took off hundreds of human lives and properties. The post-event Persistent Scatterers interferometric analysis on a stack of 20 Sentinel-1 images was performed to analyse the precursory deformations of the landslides. From the results obtained, the study region is estimated to have undergone a displacement of -26 to +19 mm/year, which indicates the instability of the terrain. Also it is evident that the occurrence of the landslides in August 2018, has been due to the effect of the torrential rainfall and the increase in the pore water inducing instability, thereby causing displacement in the region.

Keywords: PS-InSAR; Sentinel-1; landslide monitoring; remote sensing; Idukki landslide

1. Introduction

Landslides are "*the specific mass movement characterised by a down-slope movement of rock, debris, earth or a combination thereof under the influence of gravity"* (D.M.Cruden 1991; Glade and Crozier 2005; Höser 2018). The non-flat terrain exists when the resisting forces of friction and cohesion balance gravity, preventing it from flattening the terrain (Höser 2018). Concerning rainfall induced-landslides, researchers have observed and analysed various mechanisms that relate the pore pressure with slope stability. Positive pore pressure generates possible static liquefaction due to the effect of multidirectional groundwater seepage into the

soil profile (Iverson and Major 1986; Johnson and Sitar 1990; Fannin and Jaakkola 1999), while without the formation of positive pore pressures from rainfall infiltration, the failure occurs due to loss in the unsaturated shear strength with the dissipation of suction (Rahardjo et al. 2001; Collins and Znidarcic 2004). However, the environment is continuously under change, which has an impact on the occurrence of landslides on long- and short-term scales over a large or localized region. Thus, the role of preparatory, controlling and triggering factors of landslides change considerably concerning time and space, irrespective of the type and location of the landslide (Glade and Crozier 2010).

The space-borne SAR instruments provide popular widespread application because of the globally available SAR data. ERS-1, ERS-2, Sentinel-1A&B operated by the European Space Agency, JERS-1 and ALOS series operated by the National Space Development Agency of Japan, RadarSAT-1&2 operated by the Canadian Space Agency and SIR-C/X-SAR operated by the United States, Germany and Italian space agencies (Rosen et al. 2000). The data available from these satellite missions have led to the extensive utilization of SAR in varied applications. The year 1993 gave rise to a new era in geodetic measurements measuring 3-dimensional surface displacements (Simons and Rosen 2007). The deforming surface of the ice-stream in Antarctica was mapped for the first time using satellite-based InSAR technique (Goldstein et al. 1993) followed by the mapping of continuous spatial surface deformation of the 1992 Landers earthquake in the Mojave desert of southern California in the same year (Massonnet et al. 1993).

The SAR sensor detects the signal and describes it as a complex number consisting of amplitude and phase. The amplitude differentiates the types of scatterers and the topography of the terrain, whereas, the phase component contributes to the formation of the interferogram. The signal can be described as,

$$g = Ae^{-j\varphi} = Ae^{-j\frac{4\pi}{\lambda}\rho} \quad (1)$$

where g is the signal measured by the SAR sensor, A is the amplitude, *'$j\varphi$'* is the recorded phase, ρ is the slant range distance between the sensor and the respective scatterer and λ is the wavelength of the radar signal (Tom Rune Lauknes 2004; Rosen et al. 2000; Simons and Rosen 2007; Höser 2018).

Interferometry depends on the constructive or destructive interference of the electromagnetic waves from the source obtained from two different vantage points; the distance between these vantage points in the perpendicular plane to the orbit is called the interferometric baseline, and its projection perpendicular to the slant range is the perpendicular baseline. –Thus, InSAR works on the phase difference between two images of the same scene acquired from different vantage points or at different times or both (Alessandro Ferretti et al. 2007; Simons and Rosen 2007). The term 'phase' describes the path travelled twice between a target (or scatterer) and the SAR sensor by the radar pulse; this path traverses in the slant range and is dependent on it (Höser 2018) as shown below:

$$\varphi = -\frac{4\pi}{\lambda}\rho = -\frac{2\pi}{\lambda}2\rho \quad (2)$$

Where φ is the phase when the phase of the emitted signal is assumed to be zero. The negative sign indicates the phase delay of the measured signal, and *'2ρ'* denotes that the signal travels twice the distance between the antenna and target. An interferogram is formed by the complex conjugate multiplication of the slave image with the master. The interferometric phase is thus obtained, which represents the phase difference between the two SAR images, the master (φ_{mst}) and the slave (φ_{slv}) (Alessandro Ferretti et al. 2007; A Hooper, Segall, and Zebker 2007; Simons

and Rosen 2007; Höser 2018; Rosen et al. 2000). Therefore, the interferometric phase (ϕ) can be written as:

$$\phi = \varphi_{mst} - \varphi_{slv} = \frac{4\pi}{\lambda}\left(\rho_{mst} - \rho_{slv}\right) \quad (3)$$

Phase per cell in the image is a coherent sum of all the scatterers within this cell; with more scatterers, more phase noise is prone to occur. Though the radar system is independent of atmospheric disturbances (this applies only for the amplitude values), the phase signal is however influenced by the atmosphere and thereby contributes to the noises. The phase signal is also dependent on the temporal changes, and different look angles of the SAR scenes (Alessandro Ferretti et al. 2007; Plank 2014; Hanssen 2001). The cells with reliable phase values are chosen by estimating the coherence of each resolution cell; high coherence values indicate reliable phase, and it occurs in a neighbourhood without a dominant portion of noise (like double-bounce scatterers) exists (Höser 2018). Thus the interferometric phase can be represented as the composite of several components like flat earth phase (ϕ^{flat}), topographic phase (ϕ^{topo}), the displacement between two images (ϕ^{disp}), noise due to the atmosphere (ϕ^{atm}), phase contribution due to changes in platform's orbit (ϕ^{orbit}) and phase noise (ϕ^{noise}) (Hanssen 2001; Berardino et al. 2002; Crosetto et al. 2016), which can be written as:

$$\phi = \phi^{flat} + \phi^{topo} + \phi^{disp} + \phi^{atm} + \phi^{orbit} + \phi^{noise} \quad (4)$$

The isolation of the phase contribution due to displacement (ϕ^{disp}) from equation (4), by subtracting or minimizing other phase contributions, is known as the Differential InSAR (DInSAR) technique. DInSAR enables the detection of the velocity (mm/year) from the two SAR images. The Landers earthquake of 1992 demonstrated and initiated the deformation using DInSAR from the space-borne data (ERS-1) (Massonnet et al. 1993), which led to a more different and advanced 3-D measurements and time-series analysis.

Regarding landslides, the pre-failure movements cause extreme displacements at the time of the actual event, which cannot be mapped just by two images forming a single interferogram. Unlike, interferograms from earthquake event, the interferogram obtained from the landslide are too extreme to be detectable as the ϕ^{disp} signal is not dominant and obscured by other phase contributions (Andrew Hooper et al. 2012; Haghighi and Motagh 2017). These interferograms contain pure noise without any fringes or visible signs of displacements; instead, a time-series of interferograms facilitates the detection of displacement rates and shows the accelerating behaviour that leads to the landslide event (Höser 2018). The time-series approach adopts many bad interferograms, which are dominant with noise and thus, unwrapping using all of these pixels leads to wrong results. To overcome this issue, a fraction of the pixels from the image which are considered as coherent or with stable phase are equipped for phase unwrapping (Höser 2018). The concept of persistent or permanent scatterers (PS) was thus introduced (A Ferretti, Prati, and Rocca 2000; Alessandro Ferretti, Prati, and Rocca 2001). The pixels with relatively stable phase value over the whole time series were considered as the scatterers or PS, which were subsequently used for unwrapping process and displacement analysis (A Hooper, Segall, and Zebker 2007). Each target cell holds a phase value, which is the sum of all the scatterers within the cell. The persistent scatterers are target cells, which contains a single dominant scatter that maintains a stable phase over time with low variance. Thus, the changes in the phase of the persistent scatterer are said to be contributed by the dominant scatterer within the target cell, and this contributes to the precise displacement measurement (Hooper et al. 2007; Hooper et al. 2012).

Various methods exist to identify the persistent scatterers, including the SqueeSAR algorithm (Ferretti et al. 2011; Ferretti et al. 2001) and STAMPS/MTI (Stanford Method for Persistent Scatterers Multi-Temporal InSAR)(Andrew Hooper et al. 2012). The STAMPS/MTI method utilizes the amplitude and phase information of the side look data to pick the PS or DS

(Distributed Scatterers), thereby also preserving the spatial resolution of the image; a 3D phase unwrapping technique is used (Osmanoğlu et al. 2016; Höser 2018).

Several researchers have applied the time series and persistent interferometry technique, especially in landslide applications, analysing the displacement and acceleration of the targets over the years (A Hooper, Segall, and Zebker 2007; Bianchini et al. 2012; Righini, Pancioli, and Casagli 2012; Cigna, Bianchini, and Casagli 2013; Tofani et al. 2013; T. R. Lauknes et al. 2010; Bianchini et al. 2013; Osmanoğlu et al. 2016). Specific research works have provided a detailed explanation on the adoption and implementation of the STAMPS/MTI in displacement mapping (Ferretti et al. 2000; Ferretti et al. 2001; Hooper et al. 2004, 2007, 2012, 2013; Hooper 2006, 2008, 2010).

Kuriakose et al. 2009 has provided the historical data on the susceptible landslide zones in the Western Ghats region, India. Few researchers have assessed the landslide susceptible zones of the Idukki region using various slope stability techniques and probabilistic methods (Sreekumar 2009; Biju Abraham and Shaji 2013; Abraham et al. 2019). However, no research works are available for assessment of landslides using persistent scatterer interferometry in the Idukki region.

The objective of this research is to explore the possibility of identifying the unstable terrain in the landslide-prone region, which could be easily triggered at the onset of any external factors. While there are various techniques and SAR satellite systems are available to achieve this goal, there exist few drawbacks accompanied with it. The availability of satellite imagery with the high temporal resolution is the preliminary challenge, and the next hurdle arrives with the availability of a probable technique which could serve best in analysing the temporal variations in the displacement of the terrain. The S-1 imageries and the STAMPS/MTI method played a vital role in this research due to their high temporal resolution and free availability,

respectively, which produces noticeable results using the PS-InSAR technique. The research focussed on the Idukki landslide 2018, discovering the unstable spots that underwent higher displacement throughout the year and finally ending up with a significant landslide. The results illustrated the velocity of the permanent scatterers along with their respective time-series displacement trends. The highly vulnerable locations were validated using the ground verified landslide locations.

2. Description of Study Area

Idukki is one of the districts of Kerala situated in the Western Ghats of Kerala, lying in the 9.85°N latitude and 76.94°E longitude. It's the second-largest district of the state with the lowest population density. The district has a vast forest reserve, covering almost half of the district, with dense urban and sparse village settlements in villages along with tea plantations. The total area coverage of the district is 4,358 km^2, with rugged mountains and forest covering 97% of the total area; thus the district has only road access without any rail and air connectivity. Anamudi, the highest point of South India lies in the Idukki district, with thirteen other peaks exceeding the height of 2000 m. The principal rivers flowing through the district are Periyar, Thodupuzhayar, Muthirappuzhayar and Thalayar. Asia's largest dam, Idukki dam, is located in the district, where the Periyar River flows. Idukki region has a tropical climate with significant rainfall throughout the year with a short dry period. The average temperature and precipitation are 24.4℃ and 2226 mm, respectively.

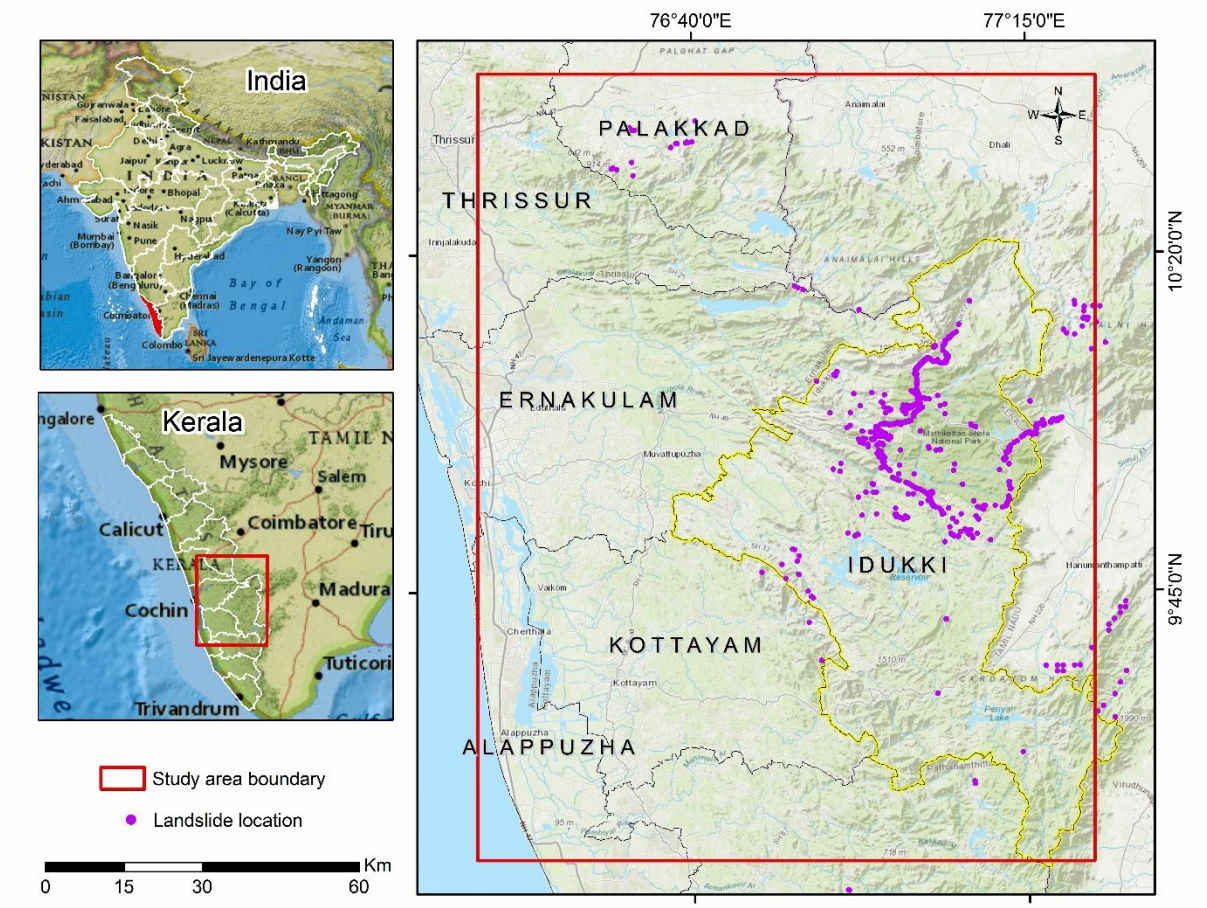

Figure 1. Location map of the study region with landslide locations.

In August 2018, the state underwent a disastrous event due to floods and landslides, creating a major catastrophe by killing many and destroying the livelihoods. Kerala received heavy monsoon rainfall, which was 116% more than the usual that led to the filling up of dams to its maximum capacity. All dams were opened due to the incessant rainfall, flooding the local low-lying areas. Out of 54 dams, 35 were opened for the first time in the state's history. The flood surplus from all five overflow gates of Idukki dam was considered being one of the main reasons which left the district panic and led to the worst scenario compared to other districts. In Idukki district, 49 died, and 11 went missing, leaving 51 people injured. Devikulam, Idukki and Udumbanchola taluks were the most affected region of the district. The devastating effect and the numerous landslide which occurred in the district made the district to be viewed as a vulnerable region, thus chosen as the study region for this study.

3. Materials and Method

Earth observation and monitoring on a global scale are facilitated, employing space-borne remote sensing data. To envision the monitoring of earth throughout the day at the time of natural calamities like floods, where the optical imageries remain incapacitated due to the presence of clouds, the SAR imageries came into play. The European Space Commission (ESA) has been providing a variety of available products called the Sentinels since 2014. The Sentinel 1A and 1B (S-1A & 1B) launched on April 2014, and April 2016 respectively are C-band (5.6 cm wavelength) SAR systems, share the same orbital plane with a 180° orbital phase difference. Both S-1A & 1B have an improved temporal resolution from twelve to six days (with two sensors functioning together), and high spatial resolution of 5 x 20 m with precise orbits has paved the way for investigating various research questions and helps in addressing numerous land applications (Intrieri et al. 2018; Höser 2018). The characteristics of the Sentinel 1A & 1B sensors are listed in table 1 (ESA 2019).

Table 1. Specifications of ESA's Sentinel-1 mission

Parameter	Sentinel 1A & 1B
Launch date	April 03, 2014 – S-1A April 22, 2016 – S-1B
Orbit type	Sun Synchronous Orbit
Orbital attitude	693 km
Repeat cycle	12 days
Sensor complement	C-SAR (5.55 cm wavelength)
Bandwidth	0 – 100 MHz
Polarization	Dual polarization for all modes (HH+HV, VV+VH)
Incidence angle range	20° - 46°
Look direction	Right
Antenna beamwidth	0.23°

Acquisition modes	Stripmap Mode (SM) Interferometric Wide swath mode (IW) Extra Wide swath mode (EW) Wave Mode (WM)
Specification of IW mode	250 km swath width 5 x 20 m spatial resolution Single-look Images three sub-swaths using TOPSAR (Terrain Observation with Progressive Scans SAR)

Since the introduction of Sentinel 1A and 1B missions, several researchers have adopted it in the analysis of surface displacements in the form of slope failures or landslides (Barra et al. 2016; Dai et al. 2016; Raspini et al. 2018; Intrieri et al. 2018; Höser 2018). The Sentinel provides data in the Interferometric Wide Swath mode so as to adopt it extensively in the InSAR technique. The IW mode captures three sub-swaths using TOPSAR, which in addition to steering the beam in range direction, also electronically steers from backward to forward in the azimuth direction for each burst, avoiding scalloping and producing homogenous image quality throughout the swath (De Zan and Guarnieri 2006; European Space Agency (ESA) 2019).

The pre-processing of Sentinel-1 images are carried out in the SNAP 7.0.0 (Sentinel Application Platform) software platform (European Space Agency 2015); also the export of processed interferograms to STAMPS/MTI (freely available)(Hooper et al. 2012; 2018) is also feasible in it, and PS processing is supported well in this platform. MATLAB is used to further modify, run and analyse the outputs from PS processing. For better visualization of the time-series output, STAMPS-Visualizer was used (Höser 2018).

The literature studies have paved a way to exploit the Sentinel 1 data efficiently to arrive with promising time series analysis on Idukki landslides. However, the current research follows a unique methodology which adopts the do's and don't's reviewed from the literature studies, providing more emphasis on the conceptual formulation of the study. Researchers have adopted the PS analysis on single bursts (Intrieri et al. 2018; Höser 2018), due to the extensive time-consumption and over-demanding hardware features, however here 7 bursts of 20 images have been taken for the analysis, which forms 19 interferograms. Figure 4 depicts the flow of the methodology adopted in the study. This chapter explains the workflow of PS process to analyse pre-movement time-series of the landslides.

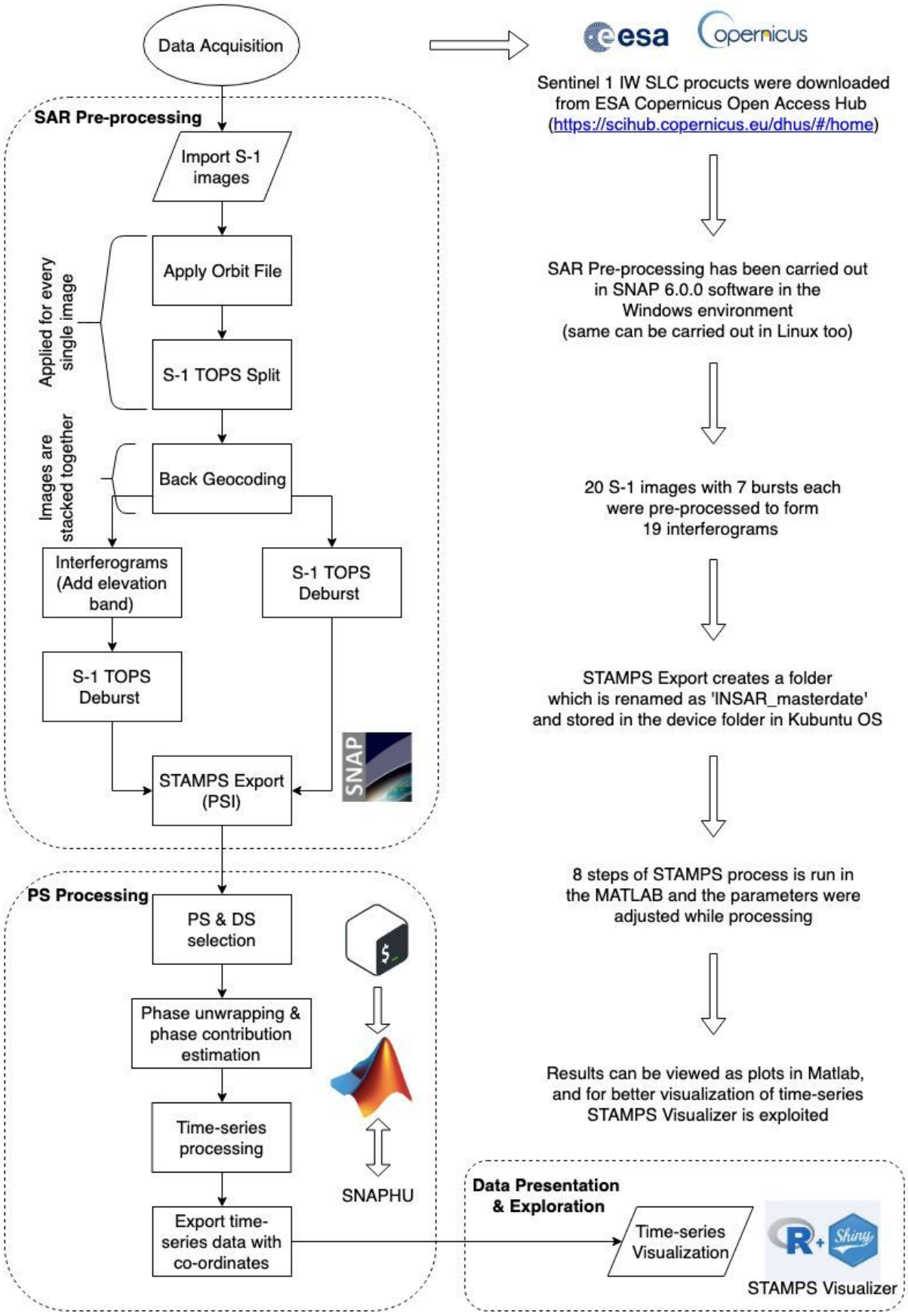

Figure 2. Flow chart of the methodology adopted in the study

The primary requirements to carry out the PS processing are a standalone computer with at least 16 GB RAM capacity; a dual operating system (OS) (a windows 10 OS dual boot with Kubuntu 18.04 was utilised for this study), with SNAP 7.0.0, MATLAB R2018a, STAMPS/MTI and R 3.4.3 software installed. The SNAP 7.0.0 along with R 3.4.3 was installed in Windows OS, while MATLAB R2018a and STAMPS/MTI were installed in the Linux OS. Though the dual handling of two software was found annoying, it provided smooth execution of the entire process. Only the MATLAB license is required for working with STAMPS/MTI, while the other Softwares mentioned could be downloaded freely, thus proving to be cost efficient in comparison to other DInSAR tools like Gamma software and SARscape (Höser 2018).

Initially, 20 Sentinel-1A IW SLC images of the study region from 23 March 2017 to 20 October 2018 were downloaded, which are available freely in the ESA's Copernicus Open Access Hub (https://scihub.copernicus.eu/dhus/#/home). The polarisation is VV, and the slopes face to the west, thus descending orbit direction was selected (Höser 2018).

The GUI (Graphical User Interface) of SNAP is quite useful in handling pre-processing procedures. The TOPS mode of data acquisition produces SLC data products in the Interferometric Wide swath mode, which could be preferably adopted in interferometric studies. The usage of TOPS provides stable signal-to-noise ratios (SNR) over the large swath of 250km, accomplishing it by splitting the swath into three sub-swaths in the range direction, which has nine bursts each in the azimuth direction (Yague-Martinez et al. 2016; Höser 2018). Every scene is thus provided as a .zip file with size up to two to five-gigabyte size, thus resulting in a massive amount of input data when 7 bursts for 20 images are in concern. The S-1 TOPS Split process separates the required region (in terms of bursts) from the entire scene. The Apply Orbit File operator downloads the information of each image, which is made available after three weeks since the image is available for download (Höser 2018). This

operator is usually carried out before the TOPS Split process. The split images are stacked together using the Back Geocoding operator; the images are co-registered to a single-master stack using the master-image-grid as the reference. The TOPS Deburst operator carries out the de-bursting process by solving the pixel overlap between the two bursts and also the void at the edges of the bursts, which arises from the sensing specifications during the TOPSAR mode of acquisition is also handled in this process. After this step, it is also feasible to subset the image further in order to reduce the size of the image.

The PS processing requires interferograms formed using the optimal master image. The Interferogram Formation operator forms single master-slave interferograms from the single-master stack, here each slave image is combined with the optimal master to provide n-1 interferograms (here, 19 interferograms are formed from 20 images). It is essential to output the elevation band along with the interferograms; the Interferogram formation operator provides a check option where the 'Output Elevation' can be checked on. The input required for PSI processing is carried out by the StaMPS Export operator. The debursted-interferograms and the debursted-back-geocoded product are given as in input to the StaMPS Export operator, which generates the input for PSI processing. This input folder is renamed as 'INSAR_masterdate' and saved in the device directory of the Kubuntu OS.

The PSI processing is done in StaMPS/MTI using an initial bash script followed by the MatLab scripts, as mentioned in the StaMPS/MTI manual (Hooper et al. 2013). The STAMPS PSI process is an eight-step procedure, which is carried out patch wise over the entire scene. At first, the phase noise is estimated for each candidate pixel in every interferogram. Based on the evaluated noise characteristics, the pixels are chosen, and the PSs are selected by accounting for the percentage of non-PS pixels in a scene. The chosen pixels are further weeded, dropping out the pixels that seem too noisy due to the contribution of neighbouring ground resolution elements. Before phase unwrapping, the selected pixels are corrected for spatially-uncorrelated

look angle error, and the patches are merged. Finally, the DEM error, master atmosphere and orbit error are eliminated from the unwrapped phase. The mean velocity and the time series plot can be viewed in MATLAB (Hooper et al. 2013, 2015).

The time-series results are exported along with the co-ordinates as a .csv file and then imported into the StaMPS-Visualizer using the Shiny package of R software to get an enhanced visualisation of the results (Höser 2018). The documentation and the manuals regarding the StaMPS-Visualizer were availed from the online scientific community 'STEP Forum', which has also provided several insights regarding the PS workflow (https://forum.step.esa.int/).

4. Results

A field expedition was carried out in September 2018 to the site after the occurrence of the landslides in August 2018; the landslide scarps were photographed, and their location was demarked. Based on the on-site visual interpretation of the landslide typologies vary from creep and subsidence to debris and avalanche along with many complex landslides. The earth/debris landslides were found common along the major corridors of the road. The vertical cuts and the sharp turnings were highly susceptible to cut-slope failures. Major events in the Idukki district were of debris flow triggered by incessant rainfall, which was also influenced by the terrain slope, land-use/land-cover and the disposition of streams.

As a result of the STAMPS procedure, the permanent scatterers are obtained. These PS points were predominantly found to be located in the region which underwent measurable displacements throughout the period. The PS of the spotted landslide scarps were identified to analyse the time-series displacement of the landslide locations.

It is to be noted that, the full potential of the ESA Sentinel constellation has not been equipped here since the acquisitions are characterised by a return period of 12 days as only Sentinel-1A acquire imagery on this study location. However, the drastic transition from historical analysis

to continuous monitoring of ground deformation at regional scales has been made feasible using satellite radar data (Intrieri et al. 2018).

StaMPS/MTI technique provided a high spatial density of measurement points (PS and DS) over the study area. Figure 3 shows the distribution of measurement points over the study area; this can be viewed in the StaMPS Visualizer (Höser 2018). As each measurement points were chosen, its time series displacement was plotted simultaneously in the side. The pattern of the PS location and the velocity (mm/year), which ranges from -25 to 15 mm/year, could be seen in the legend of Figure 3. With the trend of the plot of time series, it is possible to assess the critical situations and set up an early warning system in place, which could help evacuation possible before the disaster. However, more accuracy in the trend of time series could be obtained with an increased temporal resolution of the Sentinel images.

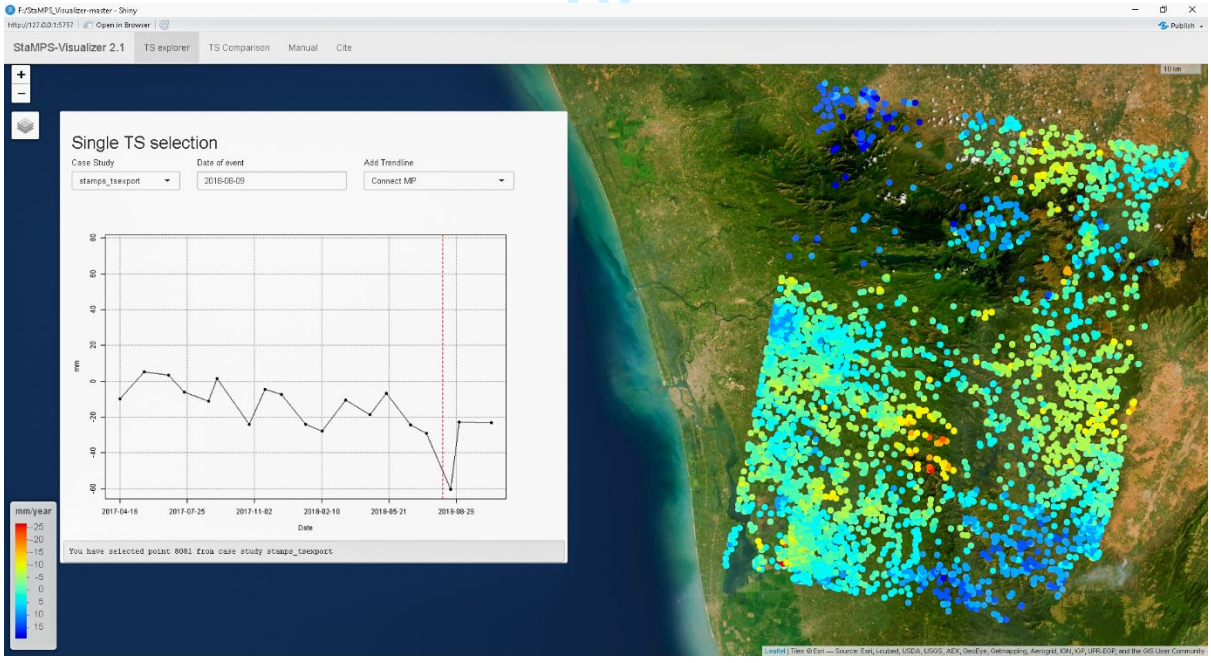

Figure 3. A view of StaMPS Visualizer window where the time series plot of each measurement points can be obtained by clicking on the individual MP's.

Numerous landslides occurred in the Idukki district on 9 August 2018; however, few of the major landslides have been demarcated on the PS processing generated resultant measurement points in figure 4 along with the corresponding images of the landslides taken at the time of a site visit. The respective time series plots of the demarcated landslides have been provided in figure 5. Figure 3 and 6 shows the distribution of the measurement points over the study region, also representing their vulnerability based on velocity using colour codes, which range from -26 to +19 mm/year. It can be inferred from the time-series plots that, there existed considerable displacements throughout the period of two years (2017 & 2018). The initial dip in the plot, which exists between the dates 25/10/2017 to 12/12/2017 represents a significant displacement at that period which also coincides with the occurrence of North-east monsoon in that region. With the increase in the downpour, the displacements are triggered. Moreover, the occurrence of the landslide on pre-occurred scarps was found to be more predominant in the region, and it is also evident from the time series plots of landslides numbered 1,2,3,4 and 5 (figure 5).

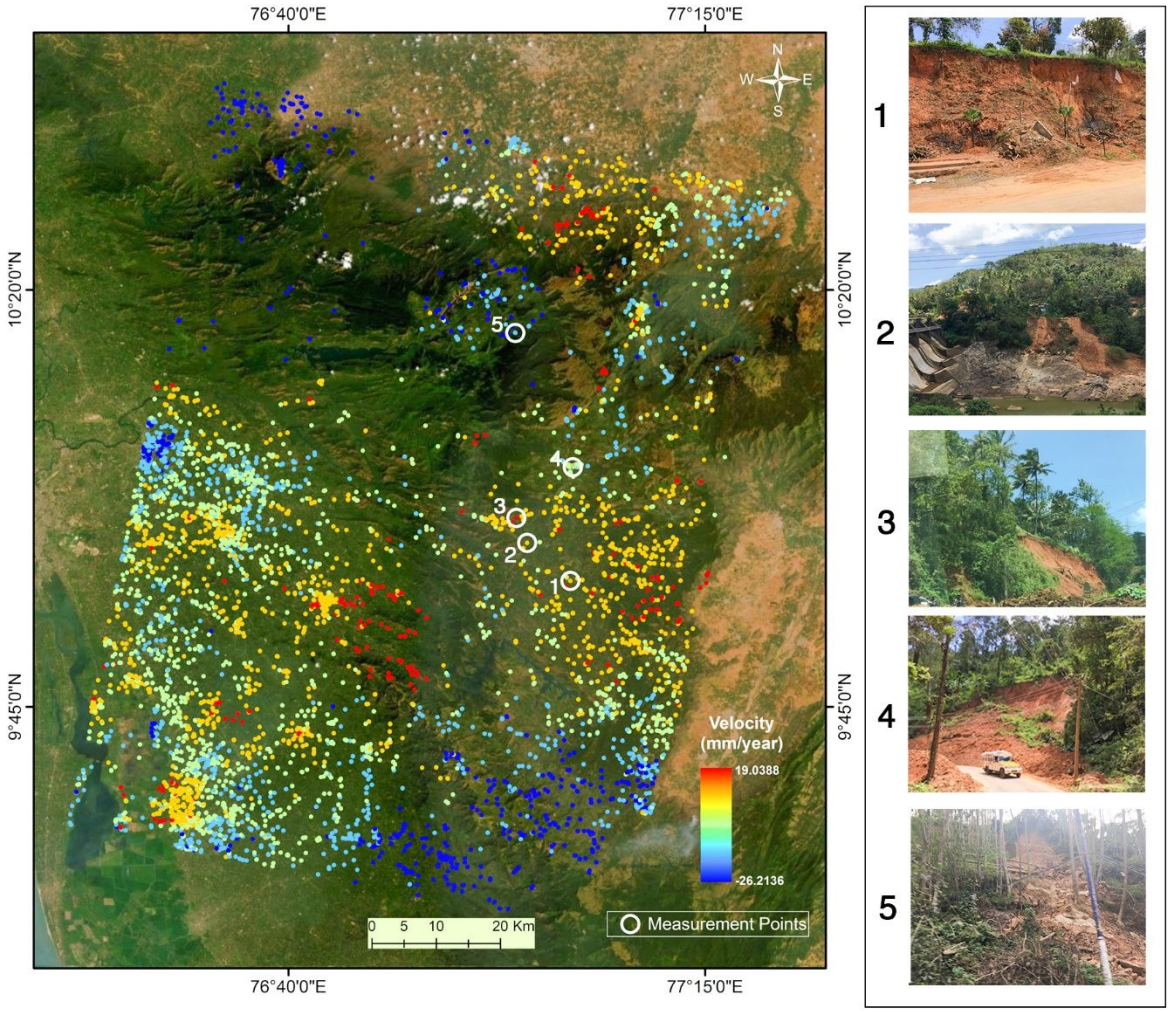

Figure 4. PS processing results of Idukki landslide. The locations of the major landslides have been marked from 1 to 5, and their corresponding images of landslide scarps have been provided. The authors took these images during the site survey in September 2018.

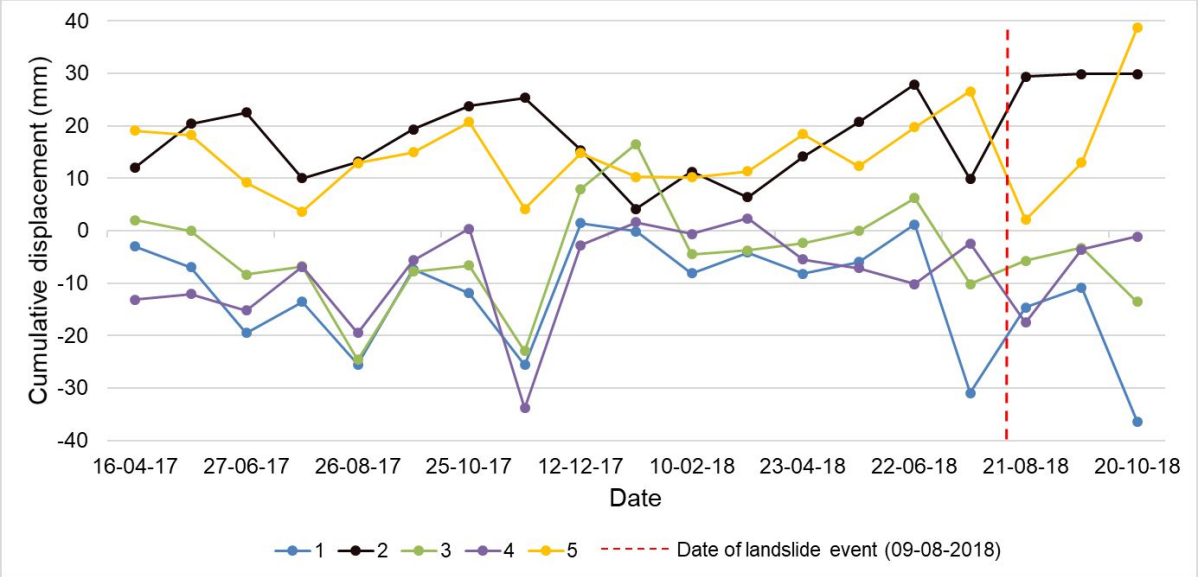

Figure 5. Time series plot of the landslides marked in figure 4; the date of the landslide event has been demarked in the plot and, notably, there is a sharp trend change at the time of the event.

5. Discussions

The Idukki district falls on the southern part of the Western Ghats where regolith thickness ranges from 0.25 to 5 m, and the region is prone to shallow landslides (Sreekumar 2009; Abraham, Pothuraju, and Satyam 2019). Geologically, the rocks in the region comprise of Charconite, Khondalite and Migmatite groups, which contributes to the formation of the part of South Indian Precambrian metamorphic shield. The terrain geomorphology of the study region divided the area into four viz., rugged hills, ridges and valley, fringe slope and plateau. The scarps of the Western Ghats are comprised of frictional soil with less cohesion, which behaves stable during dry conditions while losing their strength with the increase in its moisture content (Abraham et al. 2019). High precipitation in the region contributes to the weathering process of the rocks (Deepthy and Balakrishnan 2005).

The Western Ghats experience annual rainfall as high as 5000 mm from the southwest, northeast monsoons along with premonsoon showers (Kuriakose et al. 2009). The Western

flank and the eastern side of the Western Ghats experience landslides during the southwest monsoon and the northeast monsoon, respectively (Sekhar Lukose Kuriakose 2010). The high-intensity rainfalls increase the pore water pressure of the soil mass, leading to an eventual decrease in the shear strength of the soil. The fissures in the bedrock siphon the excess rainwater into the unstable zones in the steep terrain during the monsoon, thereby inducing landslides and debris flow (Abraham, Pothuraju, and Satyam 2019). The region underwent a breakthrough due to a quest for infrastructure because of the rapid population increase after the 19th century when the people from midlands started migrating into the hilly region (Jha, Dutt, and Bawa 2000). As an effect, significant changes in land-use occurred in a short-span favouring the occurrence of landslides. Hill-toe modifications in the district, for infrastructure development, made the slopes steep without any lateral support. These combined with terraced slopes, monoculture plantations with improper drainage provisions further aggravated the scenario.

Between 9th to 15th August to 2018, Idukki district received 679 mm of rainfall which is nearly 5.3 times more than the usual rainfall of 126.3 mm (Mishra et al. 2018). This severe, incessant rainfall, induced floods followed by landslides in the region. A significant share of landslide events was found to be biased towards the antecedent rainfall. The six out of seven major reservoirs of Kerala were at more than 90% of their full capacity before August 2018, and when followed by the extreme rainfall in August 2018, the catchment upstream of the three major reservoirs viz., Idukki, Kakki and Periyar had reached the return period of more than 500 years. The full reservoir and extreme rainfall condition resulted in the release of water from the reservoirs in a short period thus flooding the region entirely. The pore water pressure in the fully saturated soil triggered slides causing numerous landslides in the region (Mishra et al. 2018). Conclusively, the disaster in August 2018 was also due to the occurrence of torrential rainfall. The field survey and the obtained results from the PS approach coincide well, thereby

validating the authentication of the technique applied. This further concludes that the hilly slopes of Idukki district are highly vulnerable to rainfall and early warning can be provided to the locals with the onset of incessant rainfall. Furthermore, precautionary repair works have to be carried out necessarily on the landslide scarps to prevent further devastating slides over these scarps in the future.

The PS technique facilitates and agrees well with the Idukki region in mapping the time-series displacement. With more number of satellite images with a high temporal resolution, better results with well-defined trend could be obtained. Furthermore, specific landslides with high vulnerability can be analysed exclusively as the size of the image would be considerably reduced along with the processing time (as done for Maoxian landslide (Intrieri et al. 2018)). This particular research focused on carrying out the PS processing in the Idukki district, which was intensely affected during the disaster of August 2018; and hundreds of landslides occurred in the district, thus picking out of single landslide was not feasible.

The validation of results are supported by the field verified landslide locations. Figure 4 portrays the pictures obtained from the field investigation. A quantitative approach has been opted for the validation of the results, where the occurrence of landslides are well matched with the persistent scatterers, which has more velocity.

The results obtained from the STAMPS/PSI technique has been more useful in understanding the instability of the terrain. Incorporation of the triggering factors like rainfall has substantially caused considerable changes in the stability of the terrain. This study thus recommends continuous monitoring of the vulnerable region that are highly susceptible to landslides. The analysis based on the remote sensing approach is highly economical and time-consuming, which aids sufficiently in sorting the disaster management measures.

There exist few limitations in this approach which are essential to be specified. The exposition of the slope is a limiting effect. With a right looking antenna in a polar circular platform, east and west-facing slopes have proper conditions, where landslide occurs down the slope resulting in movement in LOS direction. On the other hand, in the north and south-facing slopes, the movement of landslide occur along azimuth direction, thus less chance to monitor (Alessandro Ferretti et al. 2007; Höser 2018). The PS-InSAR approach requires a high amount of data processing to arrive at the end interpretable results. Significant technical limitations are the accessibility to the hardware/software and a high amount of expert knowledge (Höser 2018). The time consumption is another limitation, but this could be addressed by taking a smaller region for the study; however, this condition only applies to study a single major landslide. If numerous landslides are under consideration, it is recommended to split the study region, and analyse each burst separately. The lack of interface between the processor and other software can be seen as another limitation; hence results are not easily revisable. Each process is carried out in each respective software, thereby making the methodology tiresome.

6. Conclusion

2018 Kerala floods and landslides was a disastrous historical event that threatened the Indian sub-continent by taking off several lives and billions of worth properties. Idukki district was immensely affected by hundreds of landslides isolating the district from the world. This deeply earned the attention of researchers, government and social activists to bring out a feasible and efficient disaster monitoring technique to mitigate the effects in the future. Freely available spaceborne radar data of Sentinel-1 system and the open-source software packages like SNAP and StaMPS/MTI along with the modern PS interferometric technique facilitated the study on the landslides effectively. The investigation of surface displacement has its history with a traditional ground measuring approach, and it has been replaced recently with the modern remote sensing tools. This evolution has paved a better path in analysing the time-series surface

displacements using the high temporal radar images. Though the precise predictions of the failure event cannot be derived from this analysis, the interpretation of the evolution and onset of preparatory and triggering factors can be assessed (Höser 2018).

The current paper gives insights into the technical and methodological concepts of time-series analysis to investigate the external factors that trigger the landslide process. However, a major focus has been given to the Idukki landslides of August 2018. The opted research methodology has provided promising insights on the stability of the region over a period of nearly 20 months including the duration of the disaster. Based on the results obtained from the study, the extreme rainfall condition accompanied by the release of water from the reservoirs in the region has made the terrain unstable making it vulnerable to landslides. Though additive factors like slope, land-use, lineaments, the flow of streams, drainage pattern, geology and geomorphology are involved in the stability of the region, rainfall has played a vital role in triggering the landslides. The proposed approach can be used preferably in the landslide susceptible region incorporating continuous monitoring to mitigate the calamitous events.

The major drawbacks are the high amount of expert knowledge required and the demanding hardware systems to run the process efficiently in a short period. The StaMPS visualizer has served as a functional interface in visualising the time-series results; however, the same can be achieved by extracting the time series information as a .csv file and analysing it separately. Therefore, the obtained results can be used to guide the authorities to detect and monitor slopes that are at the risk of failure, which is a threat to human lives and infrastructures.

Acknowledgement

No funding were obtained from any organization. We are much grateful to the European Space Agency's Copernicus Open Access Hub for providing us with Sentinel-1 images freely.

Declaration of Interest statement

The author(s) declare no competing interests.

References

Abraham, Minu Treesa, Deekshith Pothuraju, and Neelima Satyam. 2019. "Rainfall Thresholds for Prediction of Landslides in Idukki, India: An Empirical Approach." *Water (Switzerland)* 11 (10): 1–16. https://doi.org/10.3390/w11102113.

Barra, Anna, Oriol Monserrat, Paolo Mazzanti, Carlo Esposito, Michele Crosetto, and Gabriele Scarascia Mugnozza. 2016. "First Insights on the Potential of Sentinel-1 for Landslides Detection." *Geomatics, Natural Hazards and Risk*. https://doi.org/10.1080/19475705.2016.1171258.

Berardino, Paolo, Gianfranco Fornaro, Riccardo Lanari, and Eugenio Sansosti. 2002. "A New Algorithm for Surface Deformation Monitoring Based on Small Baseline Differential SAR Interferograms." *IEEE Transactions on Geoscience and Remote Sensing* 40 (11): 2375–83. https://doi.org/10.1109/TGRS.2002.803792.

Bianchini, Silvia, Francesca Cigna, Gaia Righini, Chiara Proietti, and Nicola Casagli. 2012. "Landslide HotSpot Mapping by Means of Persistent Scatterer Interferometry." *Environmental Earth Sciences* 67 (4): 1155–72. https://doi.org/10.1007/s12665-012-1559-5.

Bianchini, Silvia, Gerardo Herrera, Rosa Maria Mateos, Davide Notti, Inmaculada Garcia, Oscar Mora, and Sandro Moretti. 2013. "Landslide Activity Maps Generation by Means of Persistent Scatterer Interferometry." *Remote Sensing* 5 (12): 6198–6222. https://doi.org/10.3390/rs5126198.

Biju Abraham, P., and E. Shaji. 2013. "Landslide Hazard Zonation in and around Thodupuzha-Idukki-Munnar Road, Idukki District, Kerala: A Geospatial Approach." *Journal of the Geological Society of India* 82 (6): 649–56. https://doi.org/10.1007/s12594-013-0203-7.

Cigna, Francesca, Silvia Bianchini, and Nicola Casagli. 2013. "How to Assess Landslide Activity and Intensity with Persistent Scatterer Interferometry (PSI): The PSI-Based Matrix Approach." *Landslides* 10 (3): 267–83. https://doi.org/10.1007/s10346-012-0335-7.

Collins, Brian D., and Dobroslav Znidarcic. 2004. "Stability Analyses of Rainfall Induced Landslides." *Journal of Geotechnical and Geoenvironmental Engineering* 130 (4): 362–72. https://doi.org/10.1061/(ASCE)1090-0241(2004)130:4(362).

Crosetto, Michele, Oriol Monserrat, María Cuevas-González, Núria Devanthéry, and Bruno Crippa. 2016. "Persistent Scatterer Interferometry : A Review." *ISPRS Journal of Photogrammetry and Remote Sensing* 115: 78–89. https://doi.org/10.1016/j.isprsjprs.2015.10.011.

D.M.Cruden. 1991. "A Simple Definition of a Landslide." *Bulletin of the International Association of Engineering Geology* 43: 27–29. https://doi.org/https://doi.org/10.1007/BF02590167.

Dai, Keren, Zhenhong Li, Roberto Tomás, Guoxiang Liu, Bing Yu, Xiaowen Wang, Haiqin Cheng, Jiajun Chen, and Julia Stockamp. 2016. "Monitoring Activity at the Daguangbao Mega-Landslide (China) Using Sentinel-1 TOPS Time Series Interferometry." *Remote*

Sensing of Environment 186: 501–13. https://doi.org/10.1016/j.rse.2016.09.009.

Deepthy, R., and S. Balakrishnan. 2005. "Climatic Control on Clay Mineral Formation: Evidence from Weathering Profiles Developed on Either Side of the Western Ghats." *Journal of Earth System Science* 114 (5): 545–56. https://doi.org/10.1007/BF02702030.

ESA. 2019. "Copernicus: Sentinel-1." EO Portal Directory. 2019. https://directory.eoportal.org/web/eoportal/satellite-missions/c-missions/copernicus-sentinel-1.

European Space Agency. 2015. "SNAP Download." Science Toolbox Exploitation Platform. 2015. http://step.esa.int/main/download/snap-download/.

European Space Agency (ESA). 2019. "Interferometric Wide Swath." ESA Sentinel Online. 2019. https://sentinel.esa.int/web/sentinel/user-guides/sentinel-1-sar/acquisition-modes/interferometric-wide-swath.

Fannin, R. J., and J. Jaakkola. 1999. "Hydrological Response of Hillslope Soils above a Debris-Slide Headscarp." *Canadian Geotechnical Journal* 36 (6): 1111–22. https://doi.org/10.1139/t99-074.

Ferretti, A, C Prati, and F Rocca. 2000. "Nonlinear Subsidence Rate Estimation Using Permanent Scatterers in Differential SAR Interferometry." *IEEE Transactions on Geoscience and Remote Sensing* 38 (5): 2202–12. https://doi.org/10.1109/36.868878.

Ferretti, Alessandro, Alfio Fumagalli, Fabrizio Novali, Claudio Prati, Fabio Rocca, and Alessio Rucci. 2011. "A New Algorithm for Processing Interferometric Data-Stacks: SqueeSAR." *IEEE Transactions on Geoscience and Remote Sensing* 49 (9): 3460–70. https://doi.org/10.1109/TGRS.2011.2124465.

Ferretti, Alessandro, Andrea Monti-Guarnieri, Claudio Prati, and Fabio Rocca. 2007. *InSAR Principles: Guidelines for SAR Interferometry Processing and Interpretation*. Edited by Karen Fletcher. *ESA Publications, ESTEC, The Netherlands*. European Space Agency. https://doi.org/10.1073/pnas.81.17.5399.

Ferretti, Alessandro, Claudio Prati, and Fabio Rocca. 2001. "Permanent Scatterers in SAR Interferometry." *IEEE Transactions on Geoscience and Remote Sensing* 39 (1): 8–20. https://doi.org/10.1109/36.898661.

Glade, Thomas, and Michael J. Crozier. 2010. "Landslide Geomorphology in a Changing Environment." *Geomorphology* 120 (1–2): 1–2. https://doi.org/10.1016/j.geomorph.2009.09.018.

Glade, Thomas, and Michael J Crozier. 2005. "The Nature of Landslide Hazard Impact." In *Landslide Hazard and Risk*, edited by Thomas Glade, Malcolm Anderson, and Michael J Crozier, 41–74. John Wiley & Sons Ltd.

Haghighi, Mahmud Haghshenas, and Mahdi Motagh. 2017. "Sentinel-1 InSAR over Germany: Large-Scale Interferometry, Atmospheric Effects, and Ground Deformation Mapping." *ZFV - Zeitschrift Fur Geodasie, Geoinformation Und Landmanagement* 142 (4): 245–56. https://doi.org/10.12902/zfv-0174-2017.

Hanssen, R F. 2001. *Radar Interferometry, Data Interpretation and Error Analysis*. Edited by Freek van der Meer. Remote Sen. Kluwer Academic Publishers.

Hooper, A. 2015. "StaMPS Persistent Scatterer Exercise." *University of Leeds*.

Hooper, A, P Segall, and H Zebker. 2007. "Persistent Scatterer Interferometric Synthetic Aperture Radar for Crustal Deformation Analysis , with Application to Volcan Alcedo, Galapagos." *Journal of Geophysical Research* 112: 1–21. https://doi.org/10.1029/2006JB004763.

Hooper, Andrew. 2010. "A Statistical-Cost Approach to Unwrapping the Phase of InSAR Time Series." *Proceeding of International Workshop on ERS SAR* 2009 (March): 1–5. http://radar.tudelft.nl/~ahooper/Hooper_FRINGE_2009.pdf.

Hooper, Andrew, David Bekaert, Karsten Spaans, and Mahmut Arikan. 2012. "Recent Advances in SAR Interferometry Time Series Analysis for Measuring Crustal Deformation." *Tectonophysics* 514–517: 1–13. https://doi.org/10.1016/j.tecto.2011.10.013.

Hooper, Andrew J. 2008. "A Multi-Temporal InSAR Method Incorporating Both Persistent Scatterer and Small Baseline Approaches." *Geophysical Research Letters* 35 (16): 1–5. https://doi.org/10.1029/2008GL034654.

Hooper, Andrew John. 2006. "Persistent Scatterer Radar Interferometry for Crustal Deformation Studies and Modeling of Volcanic Deformation." Stanford University.

Hooper, Andrew, Howard Zebker, Paul Segall, and Bert Kampes. 2004. "A New Method for Measuring Deformation on Volcanoes and Other Natural Terrains Using InSAR Persistent Scatterers." *Geophysical Research Letters* 31 (October): 1–5. https://doi.org/10.1029/2004GL021737.

Hooper, Andy. 2018. "STAMPS." School of Earth and Environment, University of Leeds. 2018. https://homepages.see.leeds.ac.uk/~earahoo/stamps/.

Hooper, Andy, Karsten Spaans, David Bekaert, Miguel Caro Cuenca, and Mahmut Arıkan. 2013. *StaMPS / MTI Manual Version 3.3b1*. *School of Earth and Environment, University of Leeds*. School of Earth and Environment, University of Leeds.

Höser, Thorsten. 2018. "Analysing the Capabilities and Limitations of InSAR Using Sentinel-1 Data for Landslide Detection and Monitoring." University of Bonn.

Intrieri, Emanuele, Federico Raspini, Alfio Fumagalli, Ping Lu, Sara Del Conte, Paolo Farina, Jacopo Allievi, Alessandro Ferretti, and Nicola Casagli. 2018. "The Maoxian Landslide as Seen from Space: Detecting Precursors of Failure with Sentinel-1 Data." *Landslides*. https://doi.org/10.1007/s10346-017-0915-7.

Iverson, Richard M, and Jon J Major. 1986. "Groundwater Seepage Vectors and the Potential for Hillslope Failure and Debris Flow Mobilization." *Water Resources Research* 22 (11): 1543–48.

Jha, C. S., C. B.S. Dutt, and K. S. Bawa. 2000. "Deforestation and Land Use Changes in Western Ghats, India." *Current Science* 79 (2): 231–38.

Johnson, K. A., and N. Sitar. 1990. "Hydrologic Conditions Leading to Debris-Flow Initiation." *Canadian Geotechnical Journal* 27 (6): 789–801. https://doi.org/10.1139/t90-092.

Kuriakose, Sekhar L., G. Sankar, and C. Muraleedharan. 2009. "History of Landslide Susceptibility and a Chorology of Landslide-Prone Areas in the Western Ghats of Kerala, India." *Environmental Geology* 57 (7): 1553–68. https://doi.org/10.1007/s00254-008-1431-9.

Kuriakose, Sekhar Lukose. 2010. "Physically-Based Dynamic Modelling of the Effect of Land Use Changes on Shallow Landslide Initiation in the Western Ghats of Kerala, India." *Ph.D. Thesis, University of Utrecht, Enschede, The Netherlands*. University of Twente. https://dspace.library.uu.nl/handle/1874/188136.

Lauknes, T. R., A. Piyush Shanker, J. F. Dehls, H. A. Zebker, I. H.C. Henderson, and Y. Larsen. 2010. "Detailed Rockslide Mapping in Northern Norway with Small Baseline and Persistent Scatterer Interferometric SAR Time Series Methods." *Remote Sensing of Environment* 114 (9): 2097–2109. https://doi.org/10.1016/j.rse.2010.04.015.

Lauknes, Tom Rune. 2004. "Long-Term Surface Deformation Mapping Using Small-Baseline Differential SAR Interferograms." University of Tromso, Norway.

Massonnet, Didier, Marc Rossi, Cesar Carmona, Frederic Adragna, Gilles Peltzer, Kurt Feigl, and Thierry Rabaute. 1993. "The Displacement Field of the Landers Earthquake Mapped by Radar Interferometry." *Group* 364 (July): 138–42.

Mishra, Vimal, Saran Aadhar, Harsh Shah, Rahul Kumar, and Dushmanta Ranjan Pattanaik. 2018. "The Kerala Flood of 2018 : Combined Impact of Extreme Rainfall and Reservoir Storage," no. September: 1–13.

Osmanoğlu, Batuhan, Filiz Sunar, Shimon Wdowinski, and Enrique Cabral-Cano. 2016. "Time Series Analysis of InSAR Data: Methods and Trends." *ISPRS Journal of Photogrammetry and Remote Sensing* 115: 90–102. https://doi.org/10.1016/j.isprsjprs.2015.10.003.

Plank, Simon. 2014. "Rapid Damage Assessment by Means of Multi-Temporal SAR - A Comprehensive Review and Outlook to Sentinel-1." *Remote Sensing* 6 (6): 4870–4906. https://doi.org/10.3390/rs6064870.

Rahardjo, H., X. W. Li, D. G. Toll, and E. C. Leong. 2001. "The Effect of Antecedent Rainfall on Slope Stability." *Geotechnical and Geological Engineering* 19 (3–4): 371–99. https://doi.org/10.1023/A:1013129725263.

Raspini, Federico, Silvia Bianchini, Andrea Ciampalini, Matteo Del Soldato, Lorenzo Solari, Fabrizio Novali, Sara Del Conte, Alessio Rucci, Alessandro Ferretti, and Nicola Casagli. 2018. "Continuous, Semi-Automatic Monitoring of Ground Deformation Using Sentinel-1 Satellites." *Scientific Reports* 8: 1–11. https://doi.org/10.1038/s41598-018-25369-w.

Righini, Gaia, Valeria Pancioli, and Nicola Casagli. 2012. "Updating Landslide Inventory Maps Using Persistent Scatterer Interferometry (PSI)." *International Journal of Remote Sensing* 33 (7): 2068–96. https://doi.org/10.1080/01431161.2011.605087.

Rosen, Paul A, Scott Hensley, Ian R Joughin, Fuk K Fllk Li, Smen N Soren N Madsen, R Ernesto, Richard M I Goldstein, Ernesto Rodriguez, and Richard M I Goldstein. 2000. "Synthetic Aperture Radar Interferometry." *Proceedings of the IEEE* 20 (3): 415–74. https://doi.org/10.1007/978-3-642-11741-1_11.

Simons, M., and P. A. Rosen. 2007. "Interferometric Synthetic Aperture Radar Geodesy." In *Treatise on Geophysics*, edited by G. Schubert, Second Edi, 3:339–85. Elsevier, Amsterdam. https://doi.org/10.1016/B978-0-444-53802-4.00061-0.

Sreekumar, S. 2009. "Techniques for Slope Stability Analysis: Site Specific Studies from Idukki District, Kerala." *Journal of the Geological Society of India* 73 (6): 813–20. https://doi.org/10.1007/s12594-009-0065-1.

Tofani, Veronica, Federico Raspini, Filippo Catani, and Nicola Casagli. 2013. "Persistent

Scatterer Interferometry (PSI) Technique for Landslide Characterization and Monitoring." *Remote Sensing* 5: 1045–65. https://doi.org/10.3390/rs5031045.

Yague-Martinez, Nestor, Pau Prats-Iraola, Fernando Rodriguez Gonzalez, Ramon Brcic, Robert Shau, Dirk Geudtner, Michael Eineder, and Richard Bamler. 2016. "Interferometric Processing of Sentinel-1 TOPS Data." *IEEE Transactions on Geoscience and Remote Sensing* 54 (4): 2220–34. https://doi.org/10.1109/TGRS.2015.2497902.

Zan, Francesco De, and Andrea Monti Guarnieri. 2006. "TOPSAR: Terrain Observation by Progressive Scans." *IEEE Transactions on Geoscience and Remote Sensing* 44 (9): 2352–60. https://doi.org/10.1109/TGRS.2006.873853.